Journal of Molecular Liquids 298 (2020) 112002

Contents lists available at ScienceDirect

Journal of Molecular Liquids

journal homepage: www.elsevier.com/locate/molliq

Network of lipid interconnections at the interfaces of galactolipid and phospholipid bilayers

Robert Szczelina [b], Krzysztof Baczynski [a], Michal Markiewicz [a], Marta Pasenkiewicz-Gierula [a,*]

[a] Department of Computational Biophysics and Bioinformatics, Faculty of Biochemistry, Biophysics, and Biotechnology, Jagiellonian University, 30-387, Krakow, Poland
[b] Division of Computational Mathematics, Faculty of Mathematics and Computer Science, Jagiellonian University, 30-348, Krakow, Poland

ARTICLE INFO

Article history:
Received 27 May 2019
Received in revised form 11 September 2019
Accepted 23 October 2019
Available online 7 November 2019

Keywords:
Graph theory
Cluster size
Node strength
α-linolenoyl chain
Hydrogen bonds
Charge pairs

ABSTRACT

Interactions among lipid head groups at the bilayer/water interface do, to a large extent, determine membrane properties. In this study graph theory is employed to objectively describe and compare the pattern of the interactions at the interfaces of computer models of 128- and 512-lipid monogalactolipid (MGDG) and phosphatidylcholine (DOPC) bilayers. Both MGDG and DOPC have polar head groups but of different chemical structures so at the bilayer interfaces they participate in different types of interaction. Nevertheless, at both interfaces these interactions and the lipid molecules they link make networks. In graph theory, a network of interconnected objects (nodes) is described by well-defined quantities which define its topology and can be used to assess inner properties of the network, its strength and density, etc. In this study, several topological properties of the networks in the DOPC and MGDG bilayers are determined. A comparison of these properties indicates that the topologies of both networks differ significantly but are stable during the simulation time. The networks in the MGDG bilayers are more extended, branched, stable, and stronger than those in the DOPC bilayers. This is consistent with the smaller surface area per lipid and higher rigidity of the MGDG than the DOPC bilayers as well as the tendency of MGDG to form an inverse hexagonal phase in water. The scale of the systems is an important factor when assessing the properties of the network; the system scaling is more evident in the DOPC bilayers where several quantities increase directly proportional to the increasing size of the system than in the MGDG bilayers where this is rarely the case.

© 2019 The Authors. Published by Elsevier B.V. This is an open access article under the CC BY-NC-ND license (http://creativecommons.org/licenses/by-nc-nd/4.0/).

1. Introduction

Physicochemical studies of the lipid bilayer/water interface indicate that its properties determine the bilayer's mechanical characteristics, phase state, and permeability to water, ions, and other small molecules. Also, they determine the binding of proteins and peptides to the bilayer and affect bilayer fusion, e.g. Refs. [1–5]. As a lipid bilayer constitutes the main structural element of the biomembrane, the state of its interface affects the functioning of the membrane proteins and the overall ability of the membrane to fulfil its biological functions.

In this computational study, the interfacial regions of two types of hydrated lipid bilayer are investigated using classical molecular dynamics (MD) simulation with atomic resolution and a graph theoretical approach, and compared. One of the bilayers is composed of 1,2-di-*O*-acyl-3-*O*-β-D-galactopyranosyl-*sn*-glycerol (monogalactolipid, MGDG) with both α-linolenoyl (di-18:3-*cis*) acyl chains (MGDG bilayer); the other is composed of 1,2-dioleoyl-*sn*-glycero-3-phosphatidylcholine (DOPC bilayer). DOPC is a lamellar phase-forming lipid whereas MGDG is a non-lamellar phase-forming lipid and di-18:3-*cis* MGDG molecules upon dispersion in water spontaneously form an inverse hexagonal phase [6]. Nevertheless, in this study, the lamellar form of the MGDG mesophase is imposed by the periodic boundary conditions. A thorough discussion of the MGDG mesoscopic phases is in Ref. [7].

MGDG and DOPC have certain structural similarities as both have a glycerol backbone, two 18-carbon atom acyl chains, and at least one double bond in each chain. But MGDG and DOPC significantly differ in terms of the chemical structures of their head groups; whereas the head group of MGDG contains β-D-galactose (Fig. 1a), that of DOPC contains phosphorylcholine (Fig. 1b); both attached to the glycerol backbone. The galactose has four OH groups that are both donors and acceptors of hydrogen (H-) bonds but has no clear charge separation, only multiple small electric dipoles [8]. In contrast, the DOPC head group is zwitterionic with a negatively charged phosphate and a positively charged choline group and thus has one large electric dipole [8], but has only H-bond acceptor groups. The oxygen atoms of the glycerol backbone of DOPC and MGDG are only H-bond acceptors. The H-bond donor/acceptor capacity of the bilayer lipids strongly affects their intermolecular interactions at the bilayer/water interface e.g. Refs. [9–11] so organisation of the interface is expected to be different in the MGDG and DOPC bilayers.

* Corresponding author.
E-mail address: marta.pasenkiewicz-gierula@uj.edu.pl (M. Pasenkiewicz-Gierula).

https://doi.org/10.1016/j.molliq.2019.112002
0167-7322/© 2019 The Authors. Published by Elsevier B.V. This is an open access article under the CC BY-NC-ND license (http://creativecommons.org/licenses/by-nc-nd/4.0/).

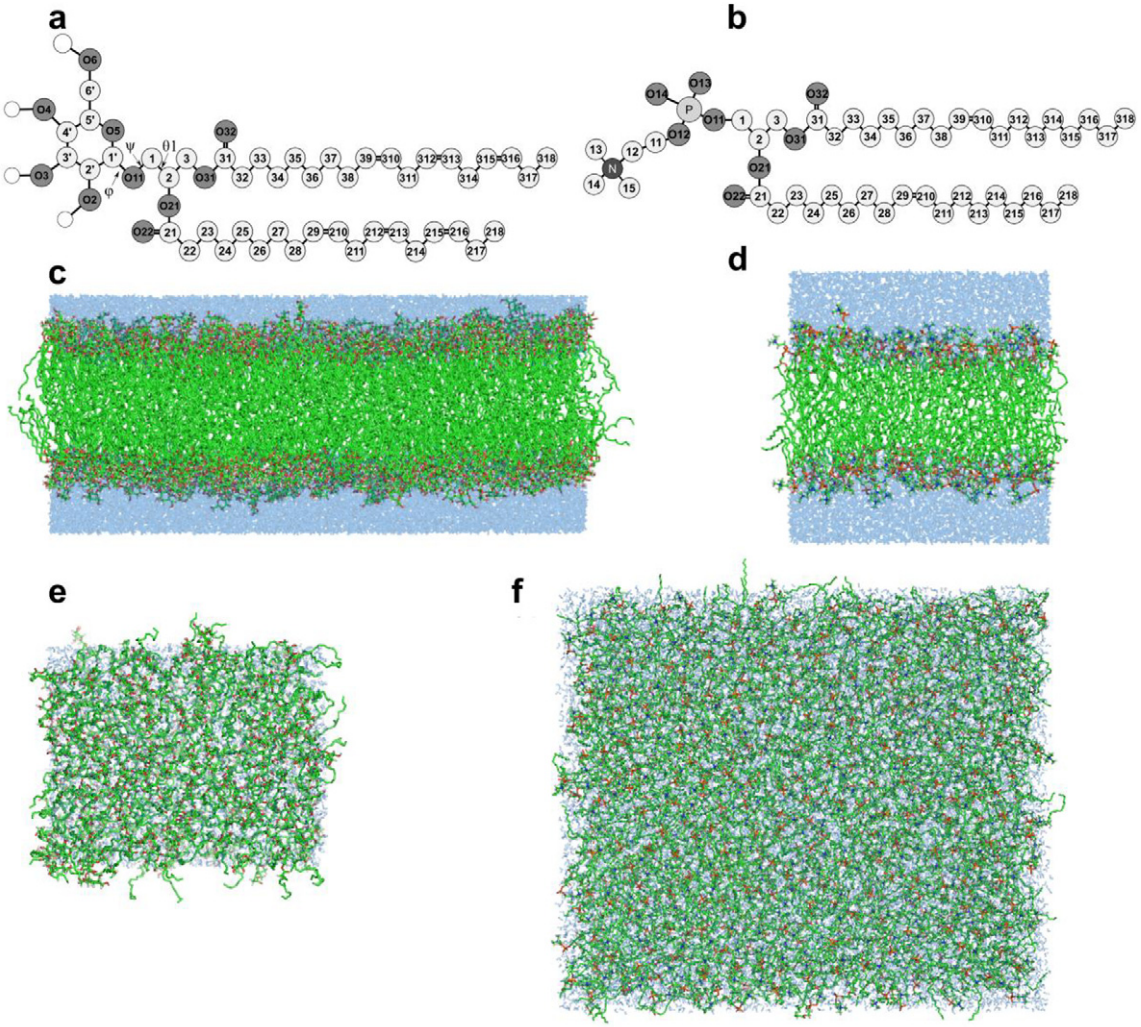

Fig. 1. The molecular structures with numbering of atoms of di-18:3 monogalactoglycerolipid (MGDG) (a) and dioleoylphosphatidylcholine (DOPC) (b). Only the polar hydrogen atoms (empty circles) of MGDG are displayed; the oxygen (O), nitrogen (N), and phosphorus (P) atoms are dark and the carbon atoms are light grey; the chemical symbol for carbon atoms, C, is omitted. Snapshots of the 4MGDG (c), DOPC (d) (side views), MGDG (e), and 4DOPC (f) (top views) bilayers at the end of their respective MD simulations. The hydrogen atoms in the acyl chains are removed to show the details of the bilayers better. The lipid atoms are coded in standard colours as sticks. The water molecules are coded in transparent blue as sticks.

As pointed out above, the acyl chains of DOPC and MGDG have the same lengths but different degrees of unsaturation (di-18:1-*cis* vs. di-18:3-*cis*). For phosphatidylcholine (PC) lipids the number of double bonds in the acyl chains has an impact on the physicochemical properties of the bilayer such as the main phase transition temperature, T_m. For the DOPC bilayer, T_m is −17 °C [12], whereas for the di-18:3-*cis* PC bilayer, T_m is between −64 and −27 °C [12]. Below T_m both bilayers are in the gel and above T_m in the liquid-crystalline lamellar phases. In contrast, di-18:3-*cis* MGDG forms an inverse hexagonal phase in water under ambient conditions and converts to a highly disordered lamellar gel phase on cooling to temperatures below −15 °C; the phase transition is very broad and low entropy [6]. Such phase behaviour is common to all unsaturated MGDG [6,13]. Therefore, the differences in the interfacial properties of the MGDG and DOPC bilayers can be attributed mainly to the differences in their head groups.

The main aim of this study is to describe the organisation of the lipid bilayer interface with a few parameters that are relatively easy to obtain. The organisation of the interface is understood as the pattern of lipid-lipid links via short-range interatomic interactions and its stability. Such a description enables some basic properties of the bilayer to be predicted and their origin to be indicated. The other aim is to assess how the results of the pattern analysis depend on the size of the simulated bilayers.

The reason for choosing the MGDG and DOPC bilayers in this study is that both DOPC and MGDG belong to main classes of lipids so the results obtained for them may be representative of the classes. Besides, the results may be helpful in understanding the mechanisms behind the formation of different mesoscopic phases when the lipids are dispersed in water in ambient conditions.

As the trajectory generated during MD simulation contains the Cartesian coordinates of each atom in the system, parameters based on geometric considerations are relatively straightforward to obtain. Therefore, in analyses of the interface organisation, to identify both the basic interatomic interactions and inter-lipid links, simple geometrical criteria are used. In classical molecular modelling, all defined interatomic interactions (bonded and non-bonded) add up to the potential energy of the system which is a function of the atomic positions only. The position of each atom in a system at a particular time is given by integrating Newton's equation of motion and results from the atoms' mutual interactions described by the potential energy function in specified simulation conditions. Thus, the pattern of interactions obtained using geometric or energetic criteria should be similar. The characteristics of the pattern can be revealed in detail via an analysis performed using a graph-theoretical approach.

The water/phosphate hydrogen-bond networks at the PC-phosphatidylglycerol (PC-PG) bilayer interface as well as their

dynamics was analysed in Ref. [14]. That detailed computational study demonstrates that linear clusters of water bridged phosphate groups can form; the clusters extend to up to six phospholipid molecules and are highly dynamic. PG is an anionic lipid and its hydroxyl groups have the potential to form intermolecular H-bonds. However, due to their negative charge, the molecules repel each other, so H-bonding is hindered. Nevertheless, these phospholipids form transient 2–3-molecule clusters via direct or water mediated H-bonds and ion-bridges [14].

The analyses using graph theory presented here are based on information concerning all types of intermolecular interactions, their average lifetimes and energies, and the number of individual interactions made by a given lipid molecule at a given time. Such an approach allowed us to describe the organisation of the interfacial regions of the bilayers which consist of vastly different lipids, such as galacto- and phospholipids, outside their biochemical context, compare them in terms of graph theory and reveal a complete picture of the inter-lipid links in this key bilayer region. Thus, a formal description of the organisation of the interface enables bilayers to be compared quantitatively and enhances the predictive power of computational methods. The predicted patterns of inter-lipid links at the MGDG and DOPC bilayer interfaces are different, which is in accord with the different tendencies of both lipids.

2. Methods

2.1. Simulation systems

Initially, two bilayers (MGDG and DOPC) were constructed manually from single MGDG and DOPC molecules (Fig. 1a and b). Each bilayer contained $8 \times 8 \times 2$ (128) lipid molecules. Details of the bilayers' constructions and MD simulations are given in Ref. [7]. Additionally, bilayers four times as large (4MGDG and 4DOPC), each containing $16 \times 16 \times 2$ (512) lipid molecules, were built by replicating the last frame of the 450-ns simulation of the MGDG and DOPC bilayers over periodic boundaries. The MGDG bilayers were hydrated with $30H_2O$/MGDG, and the DOPC bilayer was hydrated with $53H_2O$/DOPC. Even though the volume, estimated as in Ref. [15], of the DOPC phosphorylcholine moiety of 264 Å^3 is similar to that of the MGDG β-D-galactose moiety, of 243 Å^3, and the acyl chain of DOPC are monounsaturated whereas those of MGDG are triunsaturated, the surface area, A_L, per DOPC is much larger than that per MGDG (Table 1). Due to the much larger surface area a greater number of H_2O molecules/DOPC was necessary to assure the sufficient width of the water layer to prevent possible interlamellar lipid-lipid interactions via periodic boundary conditions. An exceptionally large A_L/DOPC is discussed in great detail in e.g. Refs. [16,17]. In both bilayers, the number of water molecules was significantly greater than the equilibrium number of 13–19H_2O/MGDG [18–20] and 32.5–34H_2O/DOPC [17,18]; for more details and discussion, cf. Refs [21,22]. Thorough analyses and validation of the smaller MGDG and DOPC bilayers MD simulated for 200 ns were carried out in our previous papers [7,22,23].

Table 1
Mean values for parameters describing the simulated systems.

Bilayer	DOPC	4DOPC	MGDG	4MGDG
Temperature [K]	295	295	295	295
Area [Å^2]	73.22 ± 1.22	73.43 ± 0.74	62.23 ± 0.88	61.91 ± 0.58
#Lipid···water ... H-bonds	10.55 ± 0.14	10.62 ± 0.06	9.21 ± 0.20	9.16 ± 0.12
#H-bonded water molecules	8.81 ± 0.14	8.91 ± 0.06	7.01 ± 0.17	7.08 ± 0.10
#water bridges	1.09 ± 0.09	1.07 ± 0.04	1.74 ± 0.13	1.69 ± 0.06
#H-bonds	–	–	1.04 ± 0.08	1.03 ± 0.04
#charge pairs (all)	1.44 ± 0.13	1.43 ± 0.07	–	–
Op	0.71 ± 0.09	0.71 ± 0.05	–	–
Oe	0.31 ± 0.05	0.30 ± 0.03	–	–
Oc	0.41 ± 0.07	0.41 ± 0.03	–	–

Average values of the surface area per lipid (Area); number (#) per lipid of hydrogen bonds (H-bonds) with water, H-bonded water molecules, and lipid···water···lipid... bridges, H-bonds and charge pairs, for the DOPC and MGDG bilayers MD simulated at 295 K for 450 ns and for the 4DOPC and 4MGDG bilayers additionally MD simulated for 200 ns. The errors are standard deviation estimates.

2.2. Simulation parameters and conditions

Force field parameters for the DOPC molecule as well as for the α-linolenic chain, and the glycerol moiety of the MGDG molecule, except for the partial charges on the whole DOPC head group and the MGDG glycerol backbone, were taken directly from the all-atom optimised potentials for liquid simulations (OPLS-AA) force field associated with the software package GROMACS 4 [24,25]. OPLS-AA is one of the few force fields used to simulate hydrated lipid bilayers. This force field has been refined recently to better reproduce experimental data e.g. Refs. [26–28]. The partial charges on the DOPC polar part and the MGDG glycerol backbone were taken from Ref. [29]; these charges are very similar to the CM2w charges derived in Ref. [27]. For the β-galactose moiety of MGDG, OPLS-AA parameters for carbohydrates [30] were used; these parameters were successfully tested on glycoglycerolipid bilayers in previous atomistic MD-simulation studies [7,31,32]. For water, the transferable intermolecular potential three-point model (TIP3P) was used [33]. A detailed description of the remaining simulation parameters is given in the Supporting Information (SI).

The MD simulations were carried out in the *NPT* ensemble, under a pressure of 1 atm and at a temperature of 295 K (22 °C). At this temperature, the bilayers are in the liquid-crystalline phase. The smaller bilayers were initially MD simulated for 200 ns and analysed [7] and then for 450 ns; the larger bilayers, which were assembled from the smaller ones generated in 450-ns MD simulations, were additionally MD simulated for 200 ns. The total simulation time of each larger bilayer could therefore be considered to be 650 ns. The initial 200-ns MD simulations of the smaller bilayers were extended to 450 ns to check the bilayers' stability and to check whether 100-ns equilibration was sufficient to produce well equilibrated systems. The larger bilayers were simulated and analysed to obtain better statistics and to assess the effects of the bilayer size and the simulation time on the interaction network at the bilayer interface. The first 100 ns of each MD simulation were treated as thermal equilibration. In the analyses, the last 100-ns fragments of the respective MD trajectories (between 100 and 200 ns and 350 and 450 ns of the smaller bilayers and 100 and 200 ns of the larger bilayers) were used.

Snapshots of the 4MGDG, DOPC, MGDG, and 4DOPC bilayers at the end of the respective trajectories are shown in Fig. 1c, d, e, and f.

2.3. Network analysis

Below, networks created by interactions between pairs of lipid molecules that take place at the bilayer/water interface are analysed. The most prevalent such interactions are hydrogen bonds, charge pairs, and water bridges (Fig. S1, SI). To identify these interactions, simple geometrical criteria established in Ref. [34] and applied in our previous papers [35,36] were used. The criteria are given in SI. Not all of the three types of intermolecular interaction are present in the DOPC and MGDG bilayers. As DOPC is only an H-bond acceptor, in the DOPC bilayer there are no direct inter-lipid H-bonds; however, due to the positive charge on the choline group it interacts with the negatively charged phosphate and carbonyl groups of neighbouring lipids via charge pairs [36]. This interaction most likely involves both purely electrostatic and non-conventional [37] H-bonding contributions [38], as the choline group could be considered a weak H-bond donor [39]. However, the Coulomb interaction, as the stronger one, dominates over the non-conventional H-bonding (a similar conclusion was drawn by Raveendran and Wallen for different compounds [38]) so to identify direct DOPC-DOPC interactions, H-bonding was not considered. On the contrary, MGDG is both an H-bond acceptor and donor and is able to make direct inter-lipid H-bonds but it cannot make inter-lipid charge pairs, as the galactose head group has no net charge separation. Nevertheless, both DOPC and MGDG can make H-bonds with water and a water molecule can link neighbouring lipid molecules by forming a water bridge (cf. SI). In the text below, the following abbreviations are used, Op and Oe are non-esterified and esterified, respectively, oxygen atoms of the phosphate group, Oc denotes the carbonyl oxygen atoms, and N–CH_3 is a choline methyl group (Fig. 1b).

In the bilayer interfacial region, the lipids and direct and water mediated interactions between pairs of lipids create a network of interactions. Mathematically, a network can be described and modelled by means of graph theory. A graph is a representation of a set of objects (nodes) where some pairs of the objects are connected by links (edges). Following the description proposed in Ref. [36], the nodes are the lipid molecules (centres-of-mass) in one bilayer leaflet and the edges are the intermolecular interactions among them. The terms "network" and "graph" are often used interchangeably, and when we use the term "network", we also have in mind a graph that describes this network.

A path in a graph is a list of nodes, where consecutive pairs of nodes are connected by edges. A connected component (a cluster) in a graph is a maximal subset of nodes, for which each node has a path to all other nodes in this subset. A graph is connected when it is made of only one cluster. Each graph can be decomposed into a set of maximal connected components such that there is no edge between two clusters.

A network bridge is an edge removing which disconnects the graph, thus it is the weakest network edge (cf. Fig. S2, SI). Network bridges were identified using a bridge-finding algorithm that employs chain decompositions described in Ref. [40].

Network analyses were carried out using NetworkX [41], a Python language software package for creating, manipulating, and studying the structure, dynamics, and functions of complex networks. Networks were visualised using Cytoscape [42].

In the network analysis, intermolecular H-bonds and charge pairs are counted directly as links between two molecules. However, water bridges involve both lipid and water molecules, so to calculate the number of them the scheme shown in Fig. 2 is used. Water-bridged lipids are labelled with capital letters (*A, B, C*), and H-bonds between the

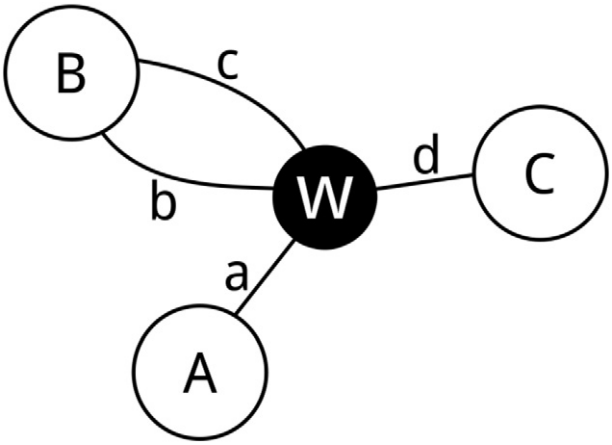

Fig. 2. Scheme showing how the numbers of intra- and intermolecular water bridges are calculated. A, B, C denote lipid molecules, and a, b, c, d denote H-bonds made with the water molecule (W).

lipids and the bridging water molecule (*W*) are labelled with lowercase letters (*a, b, c, d*). First, for each water-bridged lipid, a list with the names of the H-bonds between this lipid and the water molecule is created e.g., A:[a], B:[b,c], C:[d] (Fig. 2). The number of two-element combinations for each list corresponds to the number of intramolecular water bridges—in the example in Fig. 2, there is one intramolecular bridge, {b,c}. Then, for each pair of water-bridged lipids, a list with the names of the H-bonds between these two lipids and the water molecule is made, e.g., (A,B):[a,b,c]; (A,C): [a,d]; (B,C): [b,c,d] (Fig. 2). In the next step, for each lipid, a list of two-element combinations is made and from the list, the two-element combinations that correspond to intramolecular bridges are removed ({b,c} in Fig. 2). The remaining two-element sets are the intermolecular bridges—in the example in Fig. 2, they are {a,b}, {a,c}, {a,d}, {b,d}, {c,d}.

A network can be represented using an undirected simple graph. In a simple graph, two lipids (nodes) are considered to be connected by an edge when there is at least one intermolecular interaction between them, and two nodes can be connected only by one edge—loops (edges starting and ending at the same node, i.e. intramolecular interactions) are not allowed [43]. However, in such a description, the fact that intermolecular interactions can be of different types, the number, and relative strength (energy) is neglected. To include them, a weighted network is used (see sec. 3.2.2).

3. Results

The results obtained in sec. 3.1.1 for the smaller bilayers MD simulated for 450 ns and the larger bilayers are given in Table 1, and for the smaller bilayers MD simulated for 200 ns in Table S1 (SI).

3.1. Intermolecular interaction at the interface

3.1.1. Number of interactions

Lipid···water ... H-bonds: DOPC is only an H-bond acceptor and has fewer groups which can participate in H-bonding than MGDG which is both an H-bond donor and acceptor. Nevertheless, in the bilayer, a DOPC molecule forms more H-bonds with water and binds more water molecules than a MGDG molecule. This is because MGDG makes a significant number of lipid-lipid interactions at the bilayer interface (see below) which compete with lipid-water interactions and decrease the probability of Lipid···water ... H-bonding. The numbers of Lipid···water ... H-bonds for the smaller and larger DOPC and MGDG bilayers are given in Table 1 and Table S1 (SI).

Lipid···lipid... H-bonds: Direct Lipid···lipid... H-bonds can form only in the MGDG bilayer (cf. Fig. S1a, SI). They involve all H-bond donor and acceptor groups of the MGDG ring, glycerol backbone and carbonyl groups. The numbers of the inter-lipid H-bonds/MGDG for the MGDG and 4MGDG bilayers are given in Table 1 and Table S1 (SI).

Lipid-lipid charge pairs: Charge pairs can form only in the DOPC bilayer (cf. Fig. S1b, SI). The total numbers of charge pairs/DOPC and the numbers of charge pairs of each type for the DOPC and 4DOPC bilayers are given in Table 1 and Table S1 (SI).

Lipid-lipid water bridges: Water bridges can form both in the DOPC and MGDG bilayers (cf. Fig. S1c, SI). The numbers of Lipid···water ... lipid bridges for the smaller and larger DOPC and MGDG bilayers are given in Table 1 and Table S1 (SI).

A comparison of the entries in Table 1 and those in Table S1 (SI) indicates that the average values of interaction parameters obtained from the last 100-ns fragment of the trajectory of the system MD simulated for 200, 450, and 650 ns are practically the same and do not depend on the bilayer size. This implies that a 100 ns equilibration time of the DOPC and MGDG bilayers is sufficient to obtain representative results. As the interatomic interactions at the bilayer interface are relatively short-lived [44], 100 ns analysis time is also sufficient to obtain meaningful results. On the other hand, the dependence of the network parameters derived below on the bilayer size is not straightforward and is discussed in detail below.

3.1.2. Energy of interactions

The average energies of interatomic interactions were calculated for two distinct time frames of 100-ns trajectories of the 4DOPC and 4MGDG bilayers after equilibration as an average of the ensemble averages and were additionally averaged over particular cases of each type of interaction—in the case of H-bonding, the averaging was over that involving all H-bond donor and acceptor groups and in the case of charge pairing, over that involving the Op, Oe, and Oc oxygen atoms. The energy values are given in Table 2. As the following comparison indicates, the values are consistent with those published in the literature. The average value of the MGDG···MGDG H-bond energy of -5.12 ± 2.75 kcal/mol (Table 2) obtained in this study matches the estimated energy of galactolipid···galactolipid H-bonds in the DGDG bilayer of -5.02 ± 0.7 kcal/mol [8] very well. The energy of the charge pairing of -2.54 ± 2.16 kcal/mol (Table 2) can be compared with the energies of interactions between CO_2 and simple carbonyl compounds calculated in Ref. [38]. The net dipole moment for CO_2 is zero but CO_2 has a permanent electrical quadrupole moment [45], which results from a negative charge on each oxygen atom and a compensating positive charge on the carbon atom, distributed along the long molecular axis [46]. The interaction energies of these compounds range between −2.43 and −2.82 kcal/mol [38], thus agreement with the value obtained in this study is excellent. The binding energy of a water molecule that bridges two phosphate oxygen atoms obtained from quantum-mechanical calculations was estimated to be between 25.95 ($Op\cdots H_20\cdots Op$ bridge) and 10.37 ($Op\cdots H_20\cdots Oe$ bridge) kcal/mol, depending on which phosphate atoms (non-esterified and esterified) were bridged and what the geometry of the interacting atoms was [47]. Similar but less precise results were obtained by Pullman et al. [48]. The average energy of the $DOPC\cdots H_2O\cdots DOPC$ water bridge of -17.6 ± 6.61 kcal/mol (Table 2) is well within the range of energies obtained from quantum-mechanical calculations. Similar calculations for galactolipids are lacking, so our results cannot be compared with the published data, although the energy value of -14.23 ± 7.80 kcal/mol is reasonable because it is of a similar order to that for the DOPC water bridged interaction but slightly smaller due to smaller dipole moments of the C–O (0.20, −0.7) and O–H (−0.7, 0.43) bonds compared to those of the P-Op (1.4, −0.9) and P-Oe (1.4, −0.7) bonds. The large errors in the estimated interaction energies are due to the averaging over all groups that participate in the particular type of interactions (H-bonding, water bridging or charge pairing) and all their possible geometries at the bilayer interface.

3.2. Networks analysis

3.2.1. Simple Graph Model

To construct an undirected simple graph, a series of consecutive 10^5 networks recorded at 1ps intervals is generated:

$$(N_u^{t1}, N_d^t 1), (N_u^t 2, N_d^t 2), \ldots, (N_u^t n, N_d^t n),$$

where N_d is a network for the lower leaflet, and N_u for the upper leaflet at a given time, *tj*. From the series, the distribution of the node degrees, the size and the number of lipid clusters are estimated using the definitions below.

The degree (k_i) of the *i*-th node of a graph is the number of edges connecting this node to other nodes. The degree distribution $P(k)$ of a network is defined as the fraction of nodes in the network with degree *k*. Thus, if there are *n* nodes in the network and n_k of them have degree *k*, then $P(k) = n_k/n$. $P(k)$ allows one to establish the topology of the network analysed or in other words, the way in which different nodes are interconnected.

In network terminology, a path is an ordered series of nodes, where two consecutive nodes are connected by edges. A node (lipid) cluster is a set of interconnected nodes (there is a path from any node to any other node in a cluster) or an isolated node (a node without edges). A cluster size is the number of nodes which make a particular cluster. A cluster number is the number of clusters in the network. A network bridge (cf. Methods, sec. 2.3) is an edge in the cluster whose removal separates the cluster into two clusters (Fig. S2, SI).

Distribution of node degrees: The computed distributions of node degrees for the DOPC and MGDG bilayers are shown in Fig. 3a and b and for the 4DOPC and 4MGDG bilayers in Fig. 4a and b. The distributions suggest that in each bilayer the network has the topology of a random graph, i.e., a graph which is created by random connections among nodes [49]. Each connection is short-range as the network is created by pairs of lipid

Table 2
Average energy of interaction.

Bilayer/Interaction [kcal/mol]	DOPC	MGDG
H-bonds	–	-5.12 ± 2.75
Charge Pairs	-2.54 ± 2.16	–
Water bridges	-17.6 ± 6.61	-14.23 ± 7.80

Average energies of MGDG···MGDG H-bonds, DOPC-DOPC charge pairs, and water bridges in the 4DOPC and 4MGDG bilayers. The errors are standard deviation estimates, large error values are due to the averaging over all groups participating in the particular type of interactions and all their possible geometries at the bilayer interface.

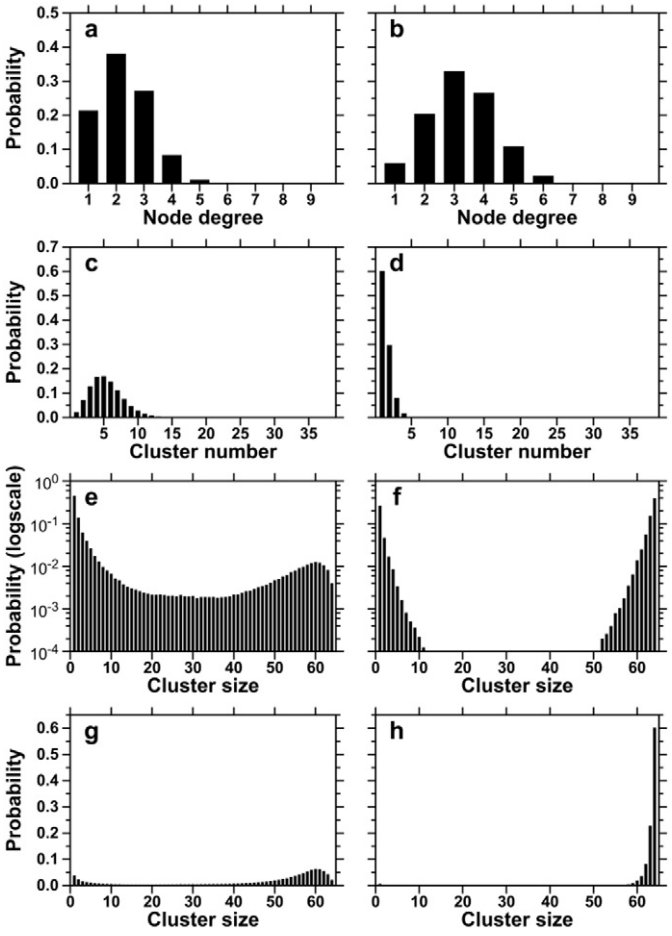

Fig. 3. Distributions of node degrees (a and b) and cluster numbers (c and d); logarithm of the probability of a cluster of a given size (e and f), probability that an arbitrarily chosen lipid molecule belongs to the cluster of a given size (g and h) in the DOPC (a, c, e, g) and MGDG (b, d, f, h) bilayers.

molecules that interact directly via H-bonds or charge pairs, and indirectly via a water molecule. These interactions are spatially limited—up to 3.25 Å, 4.0 Å, and 5.1 Å in the case of direct H-bonds, charge pairs, and water bridges, respectively, (the ranges stem from the generally accepted geometric criteria of H-bonds and charge pairs (cf. SI) [34,36]) so long-range connections are precluded. Thus, the network topology is inherited from the spatial structure of the bilayer and its dynamics and the formation of a network of different topology is rather unlikely.

In the networks of the DOPC and 4DOPC bilayers the most probable node degree is 2 (Figs. 3a and 4a); in the networks of the MGDG and 4MGDG bilayers, the most probable node degree is 3 (Figs. 3b and 4b). This means that most commonly one lipid is connected with two (DOPC) and three (MGDG), respectively, others. However, for the DOPC bilayers, node degrees 1 and 3 are also quite likely as are node degrees 2 and 4 for the MGDG bilayers.

Number and size of the lipid clusters: The probability of the partition of a node into a cluster comprising more than one node in both DOPC and both MGDG bilayers is given in Table 3. In all bilayers it is >95% and is higher in the MGDG than the DOPC bilayers. In practice, the probability does not depend on the bilayer size (Table 3).

The distributions of the numbers of clusters of interconnected lipids formed in both leaflets of the DOPC and MGDG bilayers are presented in Fig. 3c and d and Fig. 4c and d. These distributions differ significantly. For the DOPC bilayers, the numbers are relatively large and their distributions are broad, which implies that the number of possibilities for the DOPC molecules to partition into clusters in the bilayer is large. For the MGDG bilayers, the numbers are relatively small and their distributions are narrow, which indicates that the MGDG molecules partition into a much smaller number of clusters. Figs. 3c and 4c also indicate that in the DOPC and 4DOPC bilayers a single cluster comprising all lipid molecules in a bilayer leaflet rarely or never, respectively, forms. In contrast, in the MGDG and 4MGDG bilayers a single cluster (connected graph) occurs in 60% and ~11%, respectively, of cases (time frames) (Figs. 3d and 4d). The average numbers of clusters are given in Table 3. Both the averages and the standard deviations in the DOPC and 4DOPC bilayers are significantly larger than those in the MGDG and 4MGDG bilayers (Table 3).

The probabilities of the sizes of clusters (number of lipids in the cluster) that form in the DOPC and MGDG bilayers in the logarithmic scale are presented in Fig. 3e and f and Fig. 4e and f, and in the linear scale in Fig. S3 (SI). The probabilities for the smaller and larger either DOPC or MGDG bilayers are quantitatively similar but those for the MGDG bilayers differ significantly from those for the DOPC bilayers. In the MGDG bilayers, clusters of intermediate sizes do not form (Figs. 3f and 4f) whereas in both DOPC bilayers there is a whole (continuous) spectrum of sizes (Figs. 3e and 4e) with an exception for the 4DOPC bilayer where the cluster enclosing all or nearly all lipids never forms, although in the DOPC bilayers, clusters of intermediate sizes are much less probable than smaller and larger clusters (Figs. S3a, c, SI). Thus, both in the MGDG and DOPC bilayers clusters of smaller and larger sizes dominate over clusters of intermediate sizes (Fig. S3, SI). Among all cluster sizes, those including all lipid molecules constitute 0.4% and 0% of all cases in the DOPC and 4DOPC, respectively, bilayers and in 40% and 6% of all cases in the MGDG and 4MGDG, respectively, bilayers (Table 3).

In the following analysis, only the smallest and the largest clusters are considered. The average sizes of the smallest and largest clusters are given in Table 3. The average sizes of the smallest clusters in the DOPC and 4DOPC bilayers are close to one or one, respectively, whereas those in the MGDG and 4MGDG bilayers are larger with significant standard deviations. The average largest clusters in the DOPC bilayers comprise ~70–80% of the lipid molecules in a bilayer leaflet and the standard deviations of their sizes are large (Table 3). The average largest clusters in the MGDG bilayers comprise ~99% of the lipid molecules in a bilayer leaflet and the standard deviations of their sizes are small (Table 3). The time profiles of the numbers of clusters and the sizes of the smallest and largest clusters for the bilayers are shown in Figs. S4, S5, and S6 (SI), respectively. Fig. S4 (SI) shows that, in keeping with the distributions in Figs. 3c, d and 4c, d the numbers of clusters fluctuate around constant average values, the fluctuations in the DOPC bilayers are larger than in the MGDG bilayers and are also larger in the larger than smaller bilayers. Interestingly, as Fig. S5 (SI) shows, the time dependence of the size of the smallest cluster is specific to each bilayer. In the 4DOPC bilayer the size is constantly 1.0. In the other bilayers, it becomes sometimes that of the largest, as then all lipids in a bilayer leaflet belong to one cluster. This is particularly the case for the MGDG bilayer, and is consistent with the distribution of cluster numbers in Fig. 3d. Thus, except for the 4DOPC bilayer, the sizes of the smallest clusters fluctuate significantly (Fig. S5, SI). The situation is more stable for the largest cluster sizes (Fig. S6, SI). In the MGDG bilayers the sizes only slightly

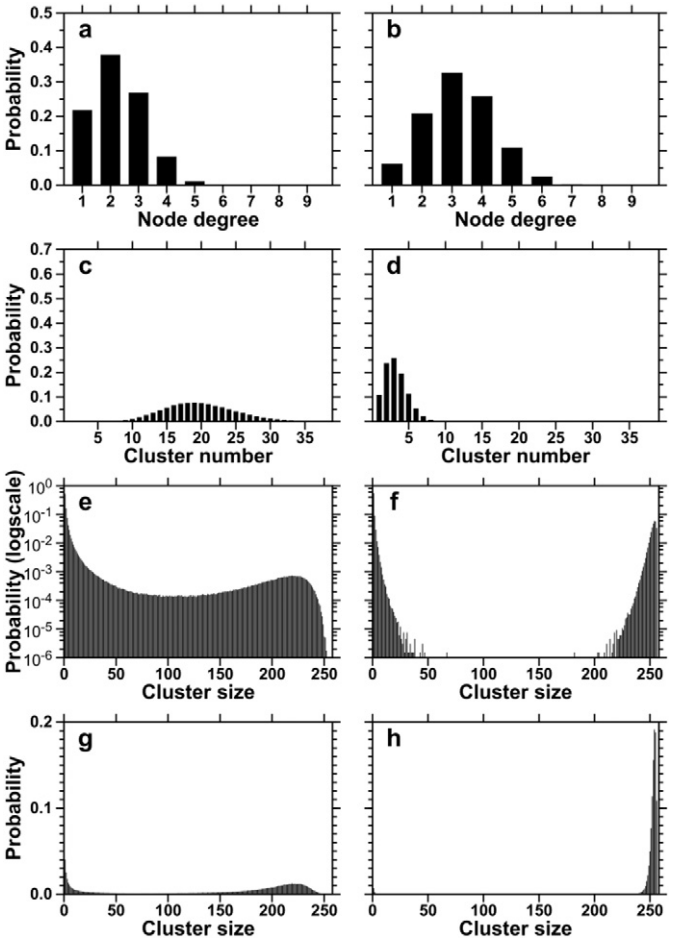

Fig. 4. Distributions of node degrees (a and b) and cluster numbers (c and d); logarithm of the probability of a cluster of a given size (e and f), probability that an arbitrarily chosen lipid molecule belongs to the cluster of a given size (g and h) in the 4DOPC (a, c, e, g) and 4MGDG (b, d, f, h) bilayers.

Table 3
Mean values of the network parameters.

Bilayer	DOPC	4DOPC	MGDG	4MGDG
		Simple Graph Model		
node probability (%)	96.15 ± 0.02	95.97 ± 0.01	99.37 ± 0.02	99.30 ± 0.01
# clusters	5.42 ± 1.75	19.90 ± 3.86	1.52 ± 0.53	3.27 ± 1.09
size smallest	2.52 ± 9.20	1.00 ± 0.00	39.05 ± 21.78	28.83 ± 56.23
size largest (%)	51.51 ± 10.67 (80.4)	186.94 ± 30.48 (73.0)	63.25 ± 0.99 (98.8)	252.80 ± 2.02 (98.7)
single cluster probability (%)	0.4	0	40	6
RP (nm)	0.21 ± 0.03	0.27 ± 0.03	0.17 ± 0.01	0.22 ± 0.02
		Weighted Graph Model		
# network bridges	27.06 ± 9.07	115.55 ± 16.36	5.12 ± 2.19	21.11 ± 4.44
node strength	23.90 ± 1.72	23.50 ± 0.94	35.25 ± 2.03	34.86 ± 0.95
		Edge lifetime [ps]		
Direct H-bonds	–	–	1.73 ± 0.005	1.73 ± 0.003
Water bridges	1.35 ± 0.005	1.35 ± 0.004	1.44 ± 0.007	1.43 ± 0.005
Op charge pairs	1.18 ± 0.003	1.17 ± 0.002	–	–
Oe charge pairs	1.18 ± 0.005	1.18 ± 0.005	–	–
Oc charge pairs	1.30 ± 0.007	1.29 ± 0.005	–	–

Simple Graph Model: probability of a node partitioning in an over-one-node cluster (node probability); average number of clusters (# clusters), size of the smallest (size smallest) and largest (size largest) clusters (in parenthesis, % of the lipids in one bilayer leaflet), probability of an all-lipid cluster (single cluster probability); time average roughness parameter (RP) of the bilayer surface; Weighted Graph Model: average number of network bridges (# network bridges), node strength (see below); average lifetimes of inter-node edges (Edge lifetime) in networks via hydrogen bonds (Direct H-bond), water bridges and N–CH_3–Oc, Op, Oe charge pairs (Oc, Op, Oe charge pairs) for the DOPC, MGDG, 4DOPC and 4MGDG bilayers MD simulated at 295 K. The errors are standard deviation estimates except for the errors in edge lifetimes which were obtained in the process of fitting each distribution of lifetimes to a single exponential function. The errors are thus fitting parameter errors and in the first approximation can be treated as standard error estimates.

fluctuate and the largest clusters mainly encompass all lipids in one bilayer leaflet (Figs. S6b, d, SI). In the 4DOPC bilayer, the largest cluster never contains all lipids (Fig. S6c, SI) and that in the DOPC bilayer occasionally includes all lipids (Fig. S6a, SI). In the DOPC bilayers fluctuations of the largest clusters sizes are significant.

To get a coherent picture of the network topology, the probabilities that an arbitrarily chosen lipid molecule belongs to a cluster of the given size in the DOPC and MGDG bilayers were calculated and are plotted in Fig. 3g and h and Fig. 4g and h. A comparison of panels e and g, as well as f and h in Figs. 3 and 4 indicates that even though the probability of finding isolated nodes in each bilayer is high, the number of lipids forming such single-molecule clusters is small and is significantly smaller in the MGDG than DOPC bilayers. The probabilities of a lipid molecule belonging to the all-lipid cluster in the DOPC, 4DOPC, MGDG, and 4MGDG bilayers, of ~2%, 0%, 60%, and ~11%, respectively (Fig. 3g and h and Fig. 4g and h), are the same as the probabilities of the single cluster forming in these bilayers (Fig. 3c and d and Fig. 4c and d), and are greater (except for the 4DOPC bilayer) than the occurrence of the all-lipid clusters in these bilayers (single cluster probability, Table 3); this is because single node probabilities there are very high, of ~45%, ~27%, ~52%, ~54%, respectively, (Fig. S3, SI).

3.2.2. Weighted graph model

To create a network of this kind, the number of individual intermolecular interactions of each type between the nodes (the pair of lipids), their average energies, and the characteristic lifetimes of the edges are assigned to each edge which connects a pair of nodes.

To determine the characteristic lifetimes of the edges, a separate network for each type of intermolecular interaction is made. The network is now a multigraph without loops where two lipids can be connected by more than one interaction and loops are not allowed. Similarly to the case of the simple graph, every 1 ps two multigraphs for each MGDG bilayer (one for intermolecular water bridges and one for direct H-bonds) and four multigraphs for each DOPC bilayer (one for intermolecular water bridges and three for charge pairs between N–CH_3 and Op, Oe, and Oc, Fig. 1) are recorded. Examples of multigraphs for the MGDG and DOPC bilayers are shown in Figs. S8 and S9 (SI). The lifetime of the connection between two nodes is an uninterrupted time during which the two nodes are connected. Distributions of the lifetimes can be considered exponential functions and to each of them a single exponent $e^{\frac{-t}{\tau}}$ with a characteristic lifetime,τ, is fitted using the least square method. Thus, for each of the networks (type of interaction), τ is determined and its value is given in Table 3. It should be borne in mind that these lifetimes are not lifetimes of particular interactions of a given type but of the edges in the network of a given type.

To calculate the weight of each edge in the weighted graph, for each multigraph a product of the number of individual interactions that account for the edge, the interaction energy and τ of the edge is calculated. The weight of each edge in the weighted graph is the sum over the multigraphs of its weights.

Examples of weighted graphs for the DOPC and the MGDG bilayer are shown in Fig. 5, where the edge colour is proportional to its weight. The dynamics of networks formed in the 4DOPC and 4MGDG bilayers is presented in films FS1 and FS2 (SI), which show that the network in the 4MGDG bilayer is significantly more extended and stable than that in the 4DOPC bilayer.

As mentioned earlier, a network bridge is the weakest edge in the cluster. The numbers of bridges in both DOPC and both MGDG bilayers are given in Table 3. The numbers of bridges in the MGDG bilayer are significantly smaller and have much smaller standard deviations than those in the DOPC bilayers. The numbers correlate very well with the dynamical behaviour of the networks in the 4DOPC and 4MGDG bilayers shown in films FS1 and FS2 (SI).

Average node strength: Node strength is the sum of the weights of the edges connected to the node. The average node strength is obtained by averaging the node strengths over all nodes in the network (in both bilayer leaflets – bilayer average) and over the analysis time (time average). The average node strengths for the networks formed in the smaller and larger DOPC and MGDG bilayers are given in Table 3.

Node strength vs time: To check the stability of the pattern of the lipid interconnection at the bilayer interface (network topology), the time profile of the average node strength is calculated and plotted in Fig. 6. For all bilayers, the plots do not show substantial time variations, which indicates that the networks have not undergone substantial reconfigurations during the 100 ns after equilibration, even though the networks themselves are of a dynamic nature.

4. Discussion

In this study, to assess the interfacial properties of the hydrated phospholipid and monogalactolipid bilayers and enable them to be compared, the following network parameters that characterise the interface were established: the probability of a lipid partitioning into an over-one-lipid cluster and to a cluster of a given size (including isolated nodes), lipid cluster number, sizes of the smallest and the largest clusters, node degree, energy of inter-lipid interactions, the number of bridges, edge lifetime, individual edge weight, and node strength. The conclusion drawn, based on the numerical values of the parameters and particularly on the node strength in the DOPC and MGDG bilayers (Table 3), is that the network of inter-lipid interactions is significantly stronger, more extended and branched in the MGDG bilayers than the DOPC bilayers, even though each acyl chain of MGDG has three double bonds, whereas that of DOPC has one double bond. This result might seem at variance with the results obtained in the study of the effect of the lipid acyl chains in saturated, mono-*cis* and mono-*trans* unsaturated PC bilayers on the properties of the bilayer interface in Ref. [50]. That study indicated that the head groups of unsaturated phospholipids bind more water molecules but make fewer inter-lipid links at the bilayer interface than those of saturated lipids. This apparent discrepancy is commented on below.

The analyses presented in this paper also allow us to assess how the parameters derived depend on the bilayer size. In this study, 128- and 512-lipid bilayers were compared. Since in both DOPC and both MGDG bilayers, the probabilities of a node partitioning into a cluster are very similar (higher than 95%, Table 3), and the node strengths in the smaller and the larger either DOPC and MGDG bilayers are also very similar (Table 3), one can expect that the network parameters for the bilayers that are four times the size are about four times as large as for the basic ones. Indeed this is true in the case of the sizes of the largest clusters and the numbers of network bridges in the bilayers as well as the numbers of clusters in the DOPC and 4DOPC bilayers (Table 3). However, there are some exceptions.

One of the exceptions is the size of the smallest cluster, which is not proportional to the number of bilayer lipids. This is because in the 4DOPC bilayer the size of the smallest cluster is constantly one, whereas in the other bilayers the sizes are very unstable and oscillate between one and even the total number of leaflet lipids (Fig. S5). This instability stems from the high probability of a lipid belonging to a cluster, a non-zero probability of just one cluster (connected graph) forming, and a high probability of isolated nodes. The other case of non-proportionality to the number of the bilayer lipids is the number of clusters in the MGDG bilayers. As Fig. 3d and h, and Figs. S5b and S6b (SI)

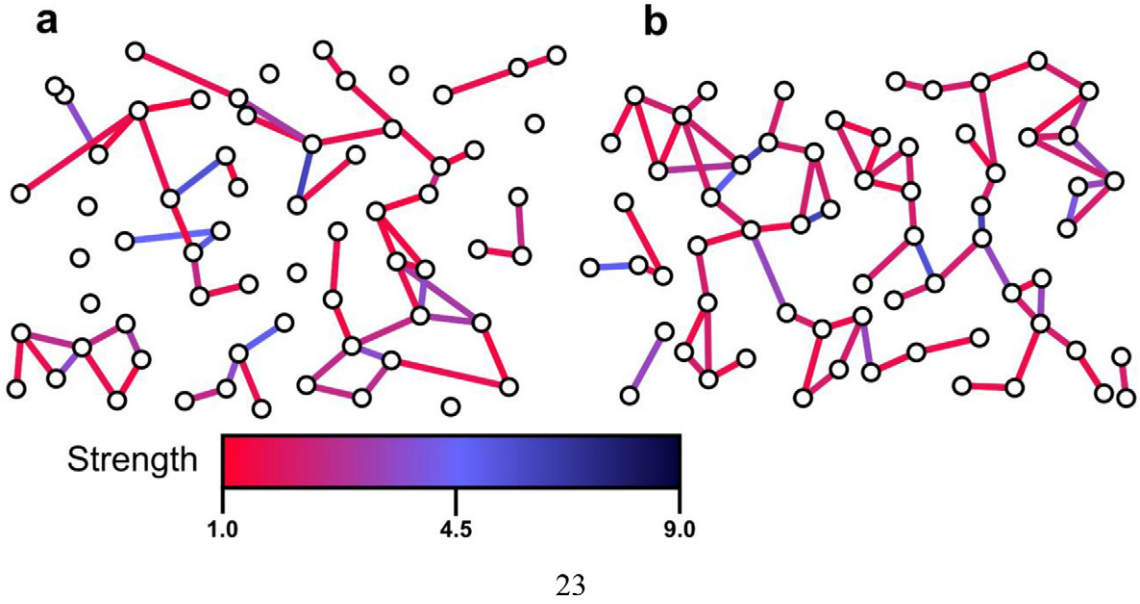

Fig. 5. Examples of weighted networks for the DOPC (a) and MGDG (b) bilayers. The colour of each edge is proportional to its weight. For clarity, edges created through periodic boundary conditions are not shown. The colour scale below codes weights of the edges (from the lowest, *light red*, to the highest, *dark blue*).

indicate, the most common situation (~60% of cases) in the MGDG bilayer is that all lipids in a bilayer leaflet are connected (form one cluster). As a result, the average number of clusters in the MGDG bilayer is ~1.5 with a small standard deviation. In the 4MGDG bilayer, lipids partition into a greater number of clusters, almost certainly because the formation of one cluster comprising all 256 lipid molecules is less likely than one comprising all 64 lipid molecules of the MGDG bilayer leaflet. Moreover, once a 256-lipid cluster forms, sustaining such a large cluster for a longer period of time is quite challenging, especially as the number of network bridges is ~20. Indeed, such a cluster persists for ~11% of the simulation time (Fig. 4d, h). But even when it disintegrates, the size of the largest cluster rarely drops below 240 lipids (Fig. S6d, SI). Thus,

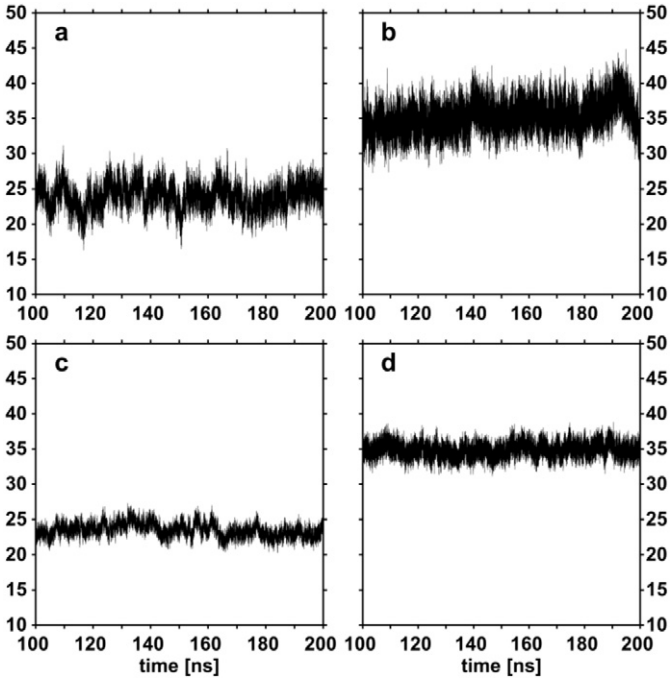

Fig. 6. Time profiles of the average node strength for the DOPC (a), MGDG (b), 4DOPC (c), and 4MGDG (d) bilayers recorded during the 100 ns after equilibration.

the network in the 4MGDG bilayer mainly consists of two, three or four clusters (Fig. 4d), of which one is of a significant size (Fig. 4h), giving an average number of clusters of ~3.2 which is twice as great as in the MGDG bilayer. Thus, with the increasing size of the bilayer the number of clusters of interconnected lipids increases and the size of the largest cluster grows proportionally to the number of bilayer lipids.

The greater number of clusters in the larger bilayers might, to some extent, be due to some instability in their surfaces. To assess this possible instability, for each bilayer an average roughness parameter (RP) [51] was calculated every 1 ps (details are given in SI). The time average values of the parameter are given in Table 3, and the time profiles of RP are shown in Fig. S7 (SI). The average RP values (Table 3) as well as its time profiles (Fig. S7, SI) indicate that the surfaces of the larger bilayers fluctuate more than those of the smaller ones. However, the effect is more pronounced in the 4DOPC (RP = 0.27 ± 0.03 nm) than in the 4MGDG (RP = 0.22 ± 0.02 nm) bilayers. Nevertheless, the roughness of the DOPC bilayer of 0.21 ± 0.03 nm is similar to that of the 4MGDG bilayer and significantly greater than that of the MGDG bilayer of 0.17 ± 0.01 nm, even though DOPC is the lamellar phase-forming lipid. Altogether, the surfaces of the DOPC bilayers fluctuate more than those of the MGDG bilayers (Fig. S7, SI). Thus, based on these results one can conclude that the number of clusters in the network of lipid interconnections at the bilayer interface is indeed to some extent related to fluctuations in the bilayer surface, but on the other hand the fluctuations bear an inverse relationship to the strength of the lipid interconnections which determine network topology. Nevertheless, any significant deformation of the 4MGDG bilayer is not observed in this simulation even though it consists of non-lamellar phase-forming lipids.

It is interesting to note that in practice the network parameters do not depend on the probability of a node partitioning into an over-one-node cluster; the high value of the probability only indicates that the probability that a lipid molecule is an isolated node is small in both DOPC and both MGDG bilayers.

On the basis of the results presented above one can draw the conclusion that in a lipid bilayer there is an optimal size of the largest lipid cluster which depends on the lipid type and the number of lipid molecules in the bilayer. In the DOPC bilayers where the lipid head groups have a lower propensity to interact with one another, the interactions among head groups in practice do not form just one cluster and the network of interactions consists of several clusters of variable sizes. In the

MGDG bilayers where the lipid head groups have a higher propensity to interact with one another, the network of interaction often consists of just one, relatively stable, cluster. However, even though the size of the largest cluster grows linearly with the number of bilayer lipids, the probability of the presence of only one cluster decreases with the number of bilayer lipids. In the DOPC bilayer the probability is ~2% (Fig. 3c, g), whereas for the 4DOPC bilayer the probability is ~0% (Fig. 4c, g); in the MGDG bilayer the probability is ~60% (Fig. 3d, h), whereas in the 4MGDG bilayer the probability is only ~11% (Fig. 4d, h).

The more branched and extended network of inter-head group interactions in the MGDG than DOPC bilayers is interrelated with the tighter packing of the MGDG than DOPC head groups at the bilayer interface reflected in a disproportionally smaller A_L per MGDG (~62 *vs.* ~73 Å^2, Table 1). From this are derived the higher order of the upper fragments of the acyl chains (above the first upper double bond) [7], the higher value of the bending rigidity modulus (31.8 ± 9.6 *vs.* 23.0 ± 3.6 kT) [7], the tendency of the MGDG to form the inverse hexagonal phase in water [6], and the only limited local motion of MGDG head groups in fast-tumbling bicelles [52]. Thus, the extended network of strong inter-lipid interactions at the MGDG bilayer interface counteracts the effect of the polyunsaturation of the MGDG acyl chains that weaken these interactions.

The network analysis of the bilayer interface presented in this paper may be helpful in linking the biological functions of a particular biomembrane to its lipid composition. This is because the properties of the membrane interface depend on the chemical structures of both the polar and nonpolar parts of the membrane lipids. On the one hand, these interfacial properties can be predicted by applying the network analysis. On the other hand, the predicted properties enable one to infer several physicochemical membrane properties that are necessary for its functions, like permeability to particular molecules, insertion and binding of certain molecules, the phase state, and others and, very importantly, reveal their atomic and molecular level origins. The latter cannot always be obtained experimentally. Thylakoid membranes can serve as an example of the connection between the interfacial properties and the membrane functions. Di-18:3 MGDG is a major constituent of the lipid matrix of thylakoid membranes which have highly curved fragments. The strong and extended network of inter-lipid interactions at the matrix interface affects surface tension and contributes to maintaining thylakoid membrane curvatures and participates in regulating the lateral pressure across the membrane to facilitate the function of membrane associated proteins, postulated in Refs. [53–55]. Moreover, as MGDG forms an inverse hexagonal phase in water spontaneously, it can also locally induce the formation of such a phase in the membrane [56]; this phase is crucial for the xanthophyll cycle [57] which is involved in protecting the photosynthetic apparatus from excess irradiation. Thus, the features of individual lipids and the physicochemical properties of the matrix which consists of these lipids are essential for the whole photosynthetic system to function correctly.

In summary, the relation between the lipid structure and the interfacial properties of the bilayer can be described formally in terms of graph theory and discriminants, such as cluster sizes/numbers and node strength/degree, which are straightforward to compute.

5. Summary

1. Computer models of the fully hydrated MGDG and DOPC bilayers of different sizes are created with MD simulation at 295 K.
2. At the bilayer interface, MGDG makes fewer H-bonds with water but more numerous direct and indirect inter-lipid interactions than DOPC.
3. The networks of inter-lipid interactions formed at the interfaces of the MGDG and DOPC bilayers are analysed using a graph-theoretical approach and compared.
4. In all bilayers, the networks have the topology of a random graph but they differ in terms of the number of lipid clusters, their sizes, the number of network bridges, and node strength.
5. The probability of lipid partitioning into an over-one-lipid cluster is in all bilayers >95% and is higher in the MGDG than DOPC bilayers. In practice the probability does not depend on the bilayer size and indicates that the probability that a lipid molecule is an isolated node is small.
6. The number of network clusters and their sizes are not connected to the probability of the node partitioning into a cluster.
7. The networks in the MGDG bilayers have fewer bridges than in the DOPC bilayers and are thus more stable.
8. In all bilayers the formation of smaller and larger clusters is much more likely than those of intermediate sizes.
9. More extended, branched, and stable MGDG clusters are consistent with the smaller surface area/lipid and higher rigidity, hence the tighter packing of the lipid head groups in the MGDG than the DOPC bilayer, and also with the tendency of MGDG to form the inverse hexagonal phase in water spontaneously.
10. In the smaller bilayers the formation of one large cluster including all leaflet lipids is more likely than in the larger bilayers.
11. 100-ns equilibration time and 100-ns analysis time of the DOPC and MGDG bilayers are sufficient to obtain representative results.

Acknowledgments

The Polish National Science Center is acknowledged for providing financial support (grant no. N301 472638). The Faculty of Biochemistry, Biophysics and Biotechnology of the Jagiellonian University is a partner of the Leading National Research Centre (KNOW), Poland supported by the Ministry of Science and Higher Education, Poland.

Appendix A. Supplementary data

Supplementary data to this article can be found online at https://doi.org/10.1016/j.molliq.2019.112002.

References

[1] E.A. Disalvo, F. Lairion, F. Martini, E. Tymczyszyn, M. Frias, H. Almaleck, G.J. Gordillo, Structural and functional properties of hydration and confined water in membrane interfaces, Biochim. Biophys. Acta Biomembr. 1778 (2008) 2655–2670.
[2] J.D. Nickels, J. Katsaras, Water and lipid bilayers, in: E.A. Disalvo (Ed.), Membrane Hydration. The Role of Water in the Structure and Function of Biological Membranes, Springer, Switzerland 2015, pp. 45–67.
[3] M. Stepniewski, A. Bunker, M. Pasenkiewicz-Gierula, M. Karttunen, T. Rog, Effects of the lipid bilayer phase state on the water membrane interface, J. Phys. Chem. B 114 (2010) 11784–11792.
[4] D. Allende, A. Vidal, S.A. Simon, T.J. McIntosh, Bilayer interfacial properties modulate the binding of amphipathic peptides, Chem. Phys. Lipids 122 (2003) 65–76.
[5] S. Ohta-Iino, M. Pasenkiewicz-Gierula, Y. Takaoka, H. Miyagawa, K. Kitamura, A. Kusumi, Fast lipid disorientation at the onset of membrane fusion revealed by molecular dynamics simulations, Biophys. J. 81 (2001) 217–224.
[6] P.W. Sanderson, W.P. Williams, Low-temperature phase behaviour of the major plant leaf lipid monogalactosyldiacylglycerol, Biochim. Biophys. Acta 1107 (1992) 77–85.
[7] K. Baczynski, M. Markiewicz, M. Pasenkiewicz-Gierula, A computer model of a polyunsaturated monogalactolipid bilayer, Biochimie 118 (2015) 129–140.
[8] M. Kanduc, A. Schlaich, A.H. de Vries, J. Jouhet, E. Marechal, B. Deme, R.R. Netz, E. Schneck, Tight cohesion between glycolipid membranes results from balanced water-headgroup interactions, Nat. Commun. 8 (2017) 14899.
[9] M. Pasenkiewicz-Gierula, K. Baczynski, M. Markiewicz, K. Murzyn, Computer modelling studies of the bilayer/water interface, Biochim. Biophys. Acta Biomembr. 1858 (2016) 2305–2321.
[10] K. Murzyn, M. Pasenkiewicz-Gierula, Structural properties of the water/membrane interface of a bilayer built of the e. Coli lipid a, J. Phys. Chem. B 119 (2015) 5846–5856.
[11] E.A. Disalvo, O.A. Pinto, M.F. Martini, A.M. Bouchet, A. Hollmann, M.A. Frias, Functional role of water in membranes updated: a tribute to trauble, Biochim. Biophys. Acta Biomembr. 1848 (2015) 1552–1562.
[12] J.R. Silvius, Thermotropic phase transitions of pure lipids in modelmembranes and their modifications by membrane proteins, in: P.C. Jost, O.H. Griffith (Eds.), Lipid-protein Interactions, John Wiley & Sons, Inc., New York 1982, pp. 239–281.

[13] W.P. Williams, The physical properties of thylakoid membrane lipids and their relation to photosynthesis, in: P.A. Siegenthaler, N. Murata (Eds.), Lipids in Photosynthesis: Structure, Function and Genetics, Kluwer Academic Publishers, The Netherlands 1998, pp. 103–118.
[14] K. Karathanou, A.N. Bondar, Dynamic water hydrogen-bond networks at the interface of a lipid membrane containing palmitoyl-oleoyl phosphatidylglycerol, J. Membr. Biol. 251 (2018) 461–473.
[15] N.R. Voss, M. Gerstein, 3v, Cavity, channel and cleft volume calculator and extractor, Nucleic Acids Res. 38 (2010) W555–W562.
[16] S. Tristram-Nagle, J.F. Nagle, Lipid bilayers: thermodynamics, structure, fluctuations, and interactions, Chem. Phys. Lipids 127 (2004) 3–14.
[17] S. Tristram-Nagle, H.I. Petrache, J.F. Nagle, Structure and interactions of fully hydrated dioleoylphosphatidylcholine bilayers, Biophys. J. 75 (1998) 917–925.
[18] R.P. Rand, V.A. Parsegian, Hydration forces between phospholipid-bilayers, Biochim. Biophys. Acta 988 (1989) 351–376.
[19] J.H. Crowe, L.M. Crowe, Lyotropic effects of water on phospholipids, in: F. Franks (Ed.), Water Science Reviews 5, Cambridge University Press 1990, pp. 1–23.
[20] I. Brentel, E. Selstam, G. Lindblom, Phase-equilibria of mixtures of plant galactolipids - the formation of a bicontinuous cubic phase, Biochim. Biophys. Acta 812 (1985) 816–826.
[21] H. Wennerstrom, E. Sparr, Thermodynamics of membrane lipid hydration, Pure Appl. Chem. 75 (2003) 905–912.
[22] K. Baczynski, M. Markiewicz, M. Pasenkiewicz-Gierula, Is the tilt of the lipid head group correlated with the number of intermolecular interactions at the bilayer interface? FEBS Lett. 592 (2018) 1507–1515.
[23] M. Markiewicz, K. Baczynski, M. Pasenkiewicz-Gierula, Properties of water hydrating the galactolipid and phospholipid bilayers: a molecular dynamics simulation study, Acta Biochim. Pol. 62 (2015) 475–481.
[24] W.L. Jorgensen, D.S. Maxwell, J. Tirado-Rives, Development and testing of the opls all-atom force field on conformational energetics and properties of organic liquids, J. Am. Chem. Soc. 118 (1996) 11225–11236.
[25] G.A. Kaminski, R.A. Friesner, J. Tirado-Rives, W.L. Jorgensen, Evaluation and reparametrization of the opls-aa force field for proteins via comparison with accurate quantum chemical calculations on peptides, J. Phys. Chem. B 105 (2001) 6474–6487.
[26] K. Murzyn, M. Bratek, M. Pasenkiewicz-Gierula, Refined opls all-atom force field parameters for n-pentadecane, methyl acetate, and dimethyl phosphate, J. Phys. Chem. B 117 (2013) 16388–16396.
[27] A. Maciejewski, M. Pasenkiewicz-Gierula, O. Cramariuc, I. Vattulainen, T. Rog, Refined opls all-atom force field for saturated phosphatidylcholine bilayers at full hydration, J. Phys. Chem. B 118 (2014) 4571–4581.
[28] W. Kulig, M. Pasenkiewicz-Gierula, T. Rog, Cis and trans unsaturated phosphatidylcholine bilayers: a molecular dynamics simulation study, Chem. Phys. Lipids 195 (2016) 12–20.
[29] P.S. Charifson, R.G. Hiskey, L.G. Pedersen, Construction and molecular modeling of phospholipid surfaces, J. Comput. Chem. 11 (1990) 1181–1186.
[30] W. Damm, A. Frontera, J. Tirado-Rives, W.L. Jorgensen, Opls all-atom force field for carbohydrates, J. Comput. Chem. 18 (1997) 1955–1970.
[31] T. Rog, I. Vattulainen, M. Karttunen, Modeling glycolipids: take one, Cell. Mol. Biol. Lett. 10 (2005) 625–630.
[32] T. Róg, I. Vattulainen, A. Bunker, M. Karttunen, Glycolipid membranes through atomistic simulations: effect of glucose and galactose head groups on lipid bilayer properties, J. Phys. Chem. B 111 (2007) 10146–10154.
[33] W.L. Jorgensen, J. Chandrasekhar, J.D. Madura, R.W. Impey, M.L. Klein, Comparison of simple potential functions for simulating liquid water, J. Chem. Phys. 79 (1983) 926–935.
[34] K. Raghavan, M.R. Reddy, M.L. Berkowitz, A molecular-dynamics study of the structure and dynamics of water between dilauroylphosphatidylethanolamine bilayers, Langmuir 8 (1992) 233–240.
[35] M. Pasenkiewicz-Gierula, Y. Takaoka, H. Miyagawa, K. Kitamura, A. Kusumi, Hydrogen bonding of water to phosphatidylcholine in the membrane as studied by a molecular dynamics simulation: location, geometry, and lipid−lipid bridging via hydrogen-bonded water, J. Phys. Chem. A 101 (1997) 3677–3691.
[36] M. Pasenkiewicz-Gierula, Y. Takaoka, H. Miyagawa, K. Kitamura, A. Kusumi, Charge pairing of headgroups in phosphatidylcholine membranes: a molecular dynamics simulation study, Biophys. J. 76 (1999) 1228–1240.
[37] Y.L. Gu, T. Kar, S. Scheiner, Fundamental properties of the ch center dot center dot center dot o interaction: is it a true hydrogen bond? J. Am. Chem. Soc. 121 (1999) 9411–9422.
[38] P. Raveendran, S.L. Wallen, Cooperative c-h--o hydrogen bonding in co2-lewis base complexes: implications for solvation in supercritical co2, J. Am. Chem. Soc. 124 (2002) 12590–12599.
[39] S.A. Pandit, D. Bostick, M.L. Berkowitz, Mixed bilayer containing dipalmitoylphosphatidylcholine and dipalmitoylphosphatidylserine: lipid complexation, ion binding, and electrostatics, Biophys. J. 85 (2003) 3120–3131.
[40] J.M. Schmidt, A simple test on 2-vertex- and 2-edge-connectivity, Inf. Process. Lett. 113 (2013) 241–244.
[41] A.A. Hagberg, D.A. Schult, P.J. Swart, Exploring network structure, dynamics, and function using networkx, in: G. Varoquaux, T. Vaught, J. Millman (Eds.),Proceedings of the 7th Python in Science Conference (SciPy2008), Pasadena, CA USA 2008, pp. 11–15.
[42] P. Shannon, A. Markiel, O. Ozier, N.S. Baliga, J.T. Wang, D. Ramage, N. Amin, B. Schwikowski, T. Ideker, Cytoscape: a software environment for integrated models of biomolecular interaction networks, Genome Res. 13 (2003) 2498–2504.
[43] R.J. Wilson, Introduction to Graph Theory, fourth ed. Addison Wesley Longman, 1996.
[44] T. Róg, K. Murzyn, J. Milhaud, M. Karttunen, M. Pasenkiewicz-Gierula, Water isotope effect on the phosphatidylcholine bilayer properties: a molecular dynamics simulation study, J. Phys. Chem. B 113 (2009) 2378–2387.
[45] A.D. Buckingham, R.L. Disch, Quadrupole moment of carbon dioxide molecule, Proc. R. Soc. Lond. Ser A Math. Phys. Sci. 273 (1963) 275–289.
[46] J.H. Williams, The molecular electric quadrupole-moment and solid-state architecture, Acc. Chem. Res. 26 (1993) 593–598.
[47] H. Frischleder, S. Gleichmann, R. Krahl, Quantum-chemical and empirical calculations on phospholipids .3. Hydration of dimethylphosphate anion, Chem. Phys. Lipids 19 (1977) 144–149.
[48] B. Pullman, A. Pullman, H. Berthod, N. Gresh, Quantum-mechanical studies of environmental effects on biomolecules .6. Ab-initio studies on hydration scheme of phosphate group, Theor. Chim. Acta 40 (1975) 93–111.
[49] P. Erdős, A. Rényi, On the evolution of random graphs, Bull. Inst. Internat. Statist 38 (1961) 343–347.
[50] K. Murzyn, T. Rog, G. Jezierski, Y. Takaoka, M. Pasenkiewicz-Gierula, Effects of phospholipid unsaturation on the membrane/water interface: a molecular simulation study, Biophys. J. 81 (2001) 170–183.
[51] E.S. Gadelmawla, M.M. Koura, T.M.A. Maksoud, I.M. Elewa, H.H. Soliman, Roughness parameters, J. Mater. Process. Technol. 123 (2002) 133–145.
[52] W.H. Ye, J. Liebau, L. Maler, New membrane mimetics with galactolipids: lipid properties in fast-tumbling bicelles, J. Phys. Chem. B 117 (2013) 1044–1050.
[53] L. Boudière, M. Michaud, D. Petroutsos, F. Rébeillé, D. Falconet, O. Bastien, S. Roy, G. Finazzi, N. Rolland, J. Jouhet, M.a. Block, E. Maréchal, Glycerolipids in photosynthesis: composition, synthesis and trafficking, Biochim. Biophys. Acta 1837 (2014) 470–480.
[54] G. Garab, B. Ughy, R. Goss, Role of mgdg and non-bilayer lipid phases in the structure and dynamics of chloroplast thylakoid membranes, in: Y. Nakamura, Y. Li-Beisson (Eds.), Lipids in Plant and Algae Development, Springer, Switzerland 2016, pp. 127–157.
[55] D. Seiwert, H. Witt, A. Janshoff, H. Paulsen, The non-bilayer lipid mgdg stabilizes the major light-harvesting complex (lhcii) against unfolding, Sci. Rep. 7 (2017) 5158.
[56] B. Deme, C. Cataye, M.A. Block, E. Marechal, J. Jouhet, Contribution of galactoglycerolipids to the 3-dimensional architecture of thylakoids, FASEB J. 28 (2014) 3373–3383.
[57] D. Latowski, H.E. Akerlund, K. Strzalka, Violaxanthin de-epoxidase, the xanthophyll cycle enzyme, requires lipid inverted hexagonal structures for its activity, Biochemistry 43 (2004) 4417–4420.